

Damage Prediction of Monolithic and Non-Monolithic Braced Unreinforced Brick Masonry Walls under Explosion Loadings

S. M. Anas^{1*}, Rayeh Nasr Al-Dala'ien^{2,3}, Mehtab Alam⁴, and Mohammad Umair¹

¹Department of Civil Engineering, Jamia Millia Islamia, 110025 New Delhi, India

²College of Graduate Studies, Universiti Tenaga Nasional, Jalan Ikram -UNITEN, 43000 Kajang, Selangor, Malaysia

³Civil Engineering Department, College of Engineering, Al-Balqa Applied University (BAU), 19117 Salt, Jordan

⁴Department of Civil Engineering, Netaji Subhas University of Technology, 110073 New Delhi, India

Abstract. Numerous unreinforced masonry (URM) structures worldwide face greater vulnerability to direct threats like earthquakes, wind, impact, or explosions compared to reinforced concrete and steel structures. Given the current worldwide environment characterized by dominance and extremism, the task of safeguarding structures, especially from explosive detonations, presents a growing and crucial obstacle for engineers and researchers. *The Masonry Society (TMS)* and the *Federal Emergency Management Agency (FEMA)* have recognized that the primary cause of material damage resulting from explosions is the collapse of walls made of URM. The recent catastrophic explosion at the Beirut seaport in Lebanon, the largest of its kind, serves as a stark reminder to town planners, architects, and structural designers. This tragic incident resulted in an immense loss of building infrastructure overall and specifically affected load-bearing masonry structures, leading to severe injuries and casualties. It underscores the urgent need for comprehensive attention and strategic measures in addressing the vulnerabilities inherent in these structures. This research study explores the response of URM walls, constructed with clay bricks, to out-of-plane blast forces. The walls are braced with either monolithic or non-monolithic transverse walls, and a three-dimensional micro-modeling approach is employed. The analysis is conducted using the Abaqus software, which utilizes the finite element method. Alongside the braced walls, the study also examines a free-standing URM wall without transverse walls. The exposed face of the walls is subjected to peak reflected pressures of 0.38 and 1.01 MPa, generated by explosive charges weighing 4.34 and 7.49 kg-TNT at scaled distances of 2.19 and 1.83 m/kg^{1/3}, respectively. The Concrete Damage Plasticity (CDP) model, which incorporates the influence of strain rate, is utilized to simulate the behavior of masonry under blast loads. Comparisons are made between the computed damage patterns of a wall reinforced with monolithic transverse walls and the experimental results found in existing literature, revealing a notable level of agreement. The influence of both monolithic and non-monolithic joints on the performance of the exposed wall is thoroughly examined and contrasted with one another, as well as with the performance of a free-standing wall. The research indicates that non-monolithic joints between the exposed wall and transverse bracing walls exhibit a greater extent of damage to the bracing walls, as this is predominantly influenced by the response of the exposed wall itself.

1. Introduction

Urban centers worldwide face the constant threat of intentional or accidental explosions. Extremist individuals, driven by radical ideologies, are increasingly resorting to targeting critical infrastructures such as government buildings, monuments, bridges, airport facilities, and embassies. Their objective is to undermine societal stability, sow chaos, and instill fear through devastating explosions [1]. Among various architectural structures, masonry load-bearing buildings are particularly vulnerable to such attacks due to their limited resistance to out-of-plane flexural forces and inherent brittleness [2]. TMS and FEMA have identified the failure of URM walls as a significant hazard to building occupants. These walls tend to disintegrate during blasts, hurling dangerous fragments and debris caused by the force of the explosion [1]. The response of a URM wall to blast loads that are applied perpendicular to its plane is predominantly determined by multiple factors. These factors include boundary conditions, slenderness ratios, the

*Corresponding author: mohdanas43@yahoo.com

placement and dimensions of openings, the ratio of opening area to wall area, as well as the wall's shear, compressive, and tensile strengths [3-7]. In a typical URM building, the walls experience two-way action when subjected to out-of-plane forces, with support provided by transverse walls on the sides and floors or roof at the top and bottom [3]. The extent of damage caused by the blast is dependent on the specific support conditions. Similar to slabs, the blast response of a URM wall supported on all four edges varies depending on whether it spans in one direction only or in both directions [3]. One-way spanning walls typically experience failure through the development of cracks that run parallel to the supports. The failure of a free-standing cantilever wall, on the other hand, depends on various factors such as the yield of the explosive, its standoff distance, the height of the explosive charge, and the location of the explosion along the length of the wall [8]. In terms of damage, horizontal cracks are more likely to occur. The formation of vertical cracks is influenced by the thickness and length to height ratio of the wall. However, walls that span in both directions primarily fail by developing diagonal cracking, accompanied by sparse vertical cracks near the supporting edges [3]. The behavior of masonry walls is further complicated by inherent heterogeneity resulting from the use of queen closer, three-quarter bat, and workmanship during construction [1-3, 8-9]. This complexity adds to the challenges faced in understanding and analyzing the behavior of these walls. Thorough research and analysis are necessary to mitigate potential threats and ensure the safety and stability of infrastructure.

Numerous analyses, both computational and experimental, have been carried out to study the repercussions and blast effects on the structural elements of buildings [2, 8-13]. These investigations typically involve strain rates exceeding 1 /s, while quasi-static testing involves strain rates ranging from 10^{-5} to 10^{-7} /s. However, further research is necessary due to the presence of significant nonlinear behavior and the potential for brittle failure, which makes it challenging to accurately simulate the impact of explosions. Numerous studies have emphasized the risk of fatalities and the vulnerability of masonry envelopes to out-of-plane loading, particularly in the context of earthquakes [14-16, 17-19] and explosion debris [8-13]. It is crucial to delve deeper into these areas to gain a comprehensive understanding of their implications for infrastructure safety and design. Explosions have distinct effects on a building's external structure, but earthquake-resistant buildings are unlikely to be impacted in the same way. This disparity is due to several factors, such as the difference between explosions directly affecting the building's exterior while earthquakes originate from movements at the foundation. Explosions usually result in limited damage in a specific area, while earthquakes elicit a worldwide reaction. Surprisingly, there is a dearth of laboratory experiments that replicate scenarios involving car collisions with parapets and air blasts, as found in existing literature [20-21].

The velocity at which deformation occurs is of utmost importance in dictating the mechanical response of constructions subjected to explosive circumstances. Explosions typically generate strain rates ranging from 10^2 to 10^4 /s [8-13, 22-24]. This phenomenon significantly affects structures constructed with reinforced concrete. Their resistance can experience a substantial increase, with documented dynamic increase factors of up to 4 for compression and 6 for tension [22]. However, research on masonry and its components is limited. Recent studies have revealed dynamic increase factors exceeding 2 for compression in clay brick structures [22]. These findings highlight the importance of understanding and mitigating the effects of strain rate on different construction materials to ensure the safety and integrity of infrastructure.

The blast resistance of building components is an area of research that lacks experimental data due to several factors. These factors include the difficulty in accessing test locations, the expensive nature of specimen transportation, the requirement to rent specialized equipment for conducting experiments, and the inherent hazards associated with testing explosions. Consequently, there is a significant dearth of empirical studies in this field. [13, 17, 25]. The constraints in place impose limitations on the quantity of tests that can be performed, as well as the scope of parameters that can be analyzed within each testing regimen. Nevertheless, advancements in computer hardware and software technologies have given rise to numerical modeling as a viable and economical substitute for explosive field testing. This alternative approach offers practicality and cost-effectiveness [25]. Using numerical modeling, researchers now have the opportunity to thoroughly investigate various design factors at a significantly lower cost [25]. This approach offers a viable solution for studying blast resistance in-depth while mitigating the risks and constraints associated with traditional experimental methods.

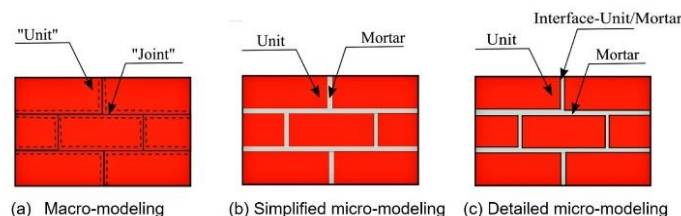


Fig. 1. Different approaches to modeling in masonry construction

A widely used and versatile finite element software called Abaqus is employed to simulate and study the impact of air-blast loading on masonry walls without reinforcement. This article considers various factors such as the nonlinear behavior of bricks and mortar joints, the occurrence of cracks, and the interactions between the bricks and mortar. The aim is to analyze and understand the effects of air-blast loading on unreinforced brick masonry walls using a comprehensive physics-based approach provided by Abaqus.

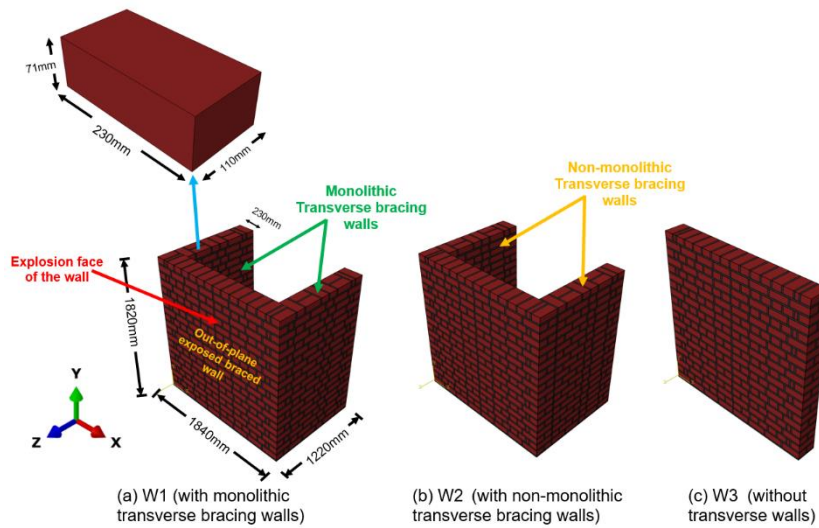


Fig. 2. The FEM models created within the Abaqus

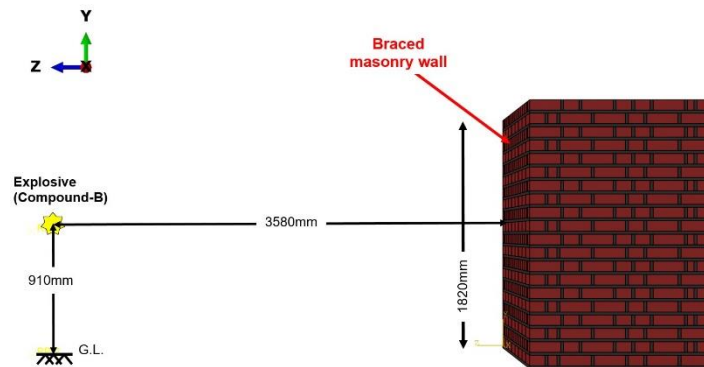


Fig. 3. Explanation of the explosive's location: a situation where the explosion is not contained

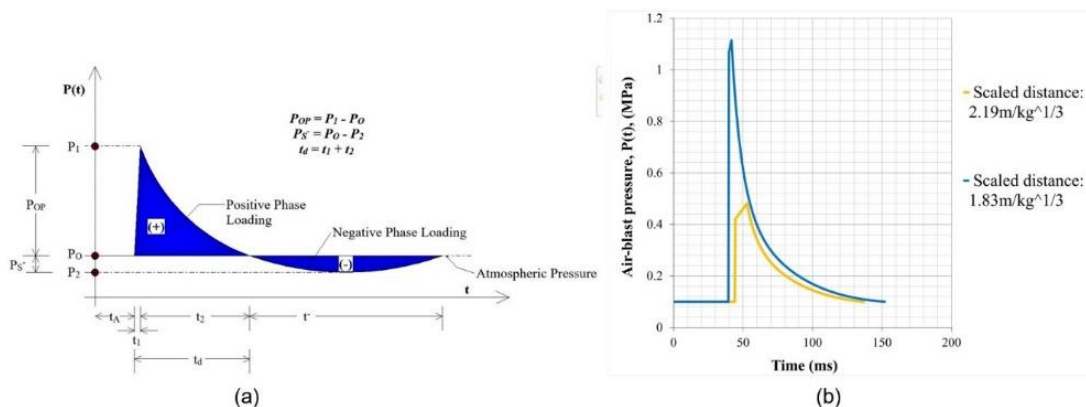


Fig. 4. (a) blast profile that is idealized; and (b) pressure profiles that have been computed through experimentation

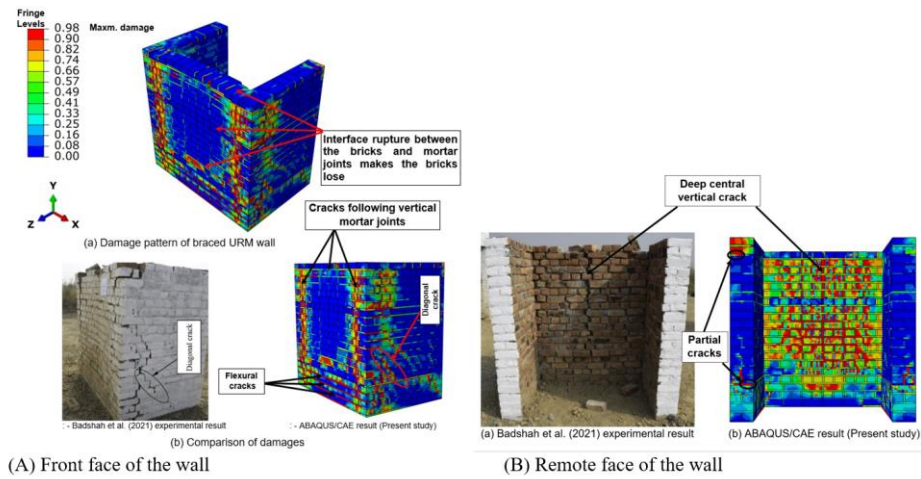


Fig. 5. Damages at $2.19\text{m/kg}^{1/3}$ ($t=137\text{ms}$)

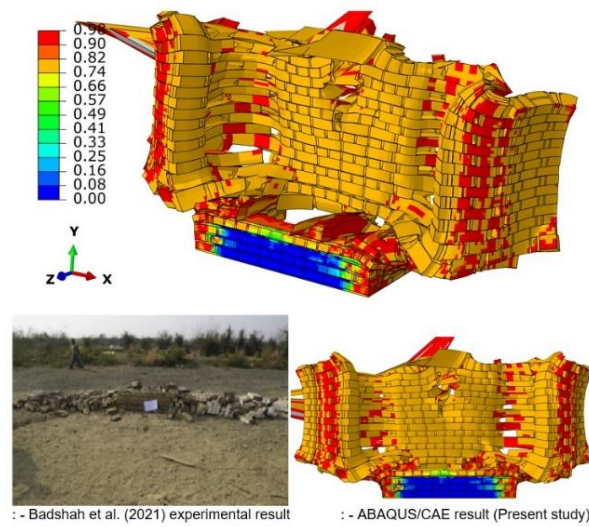


Fig. 6. Damages at $1.83\text{m/kg}^{1/3}$ ($t=152\text{ms}$)

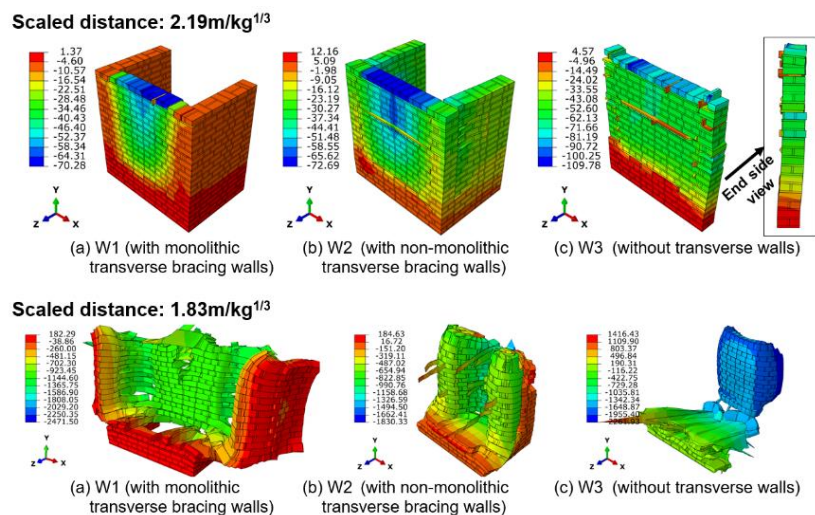
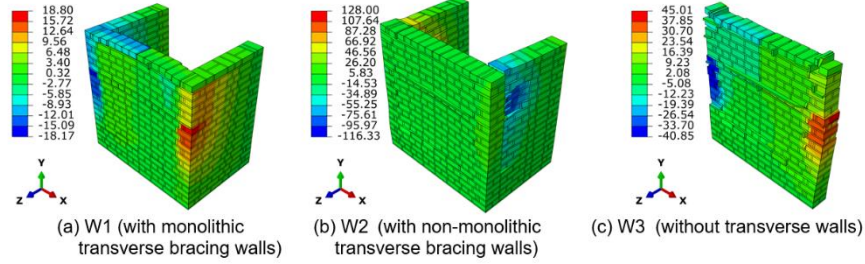


Fig. 7. Z-displacement (mm) contours

Scaled distance: $2.19\text{m/kg}^{1/3}$



Scaled distance: $1.83\text{m/kg}^{1/3}$

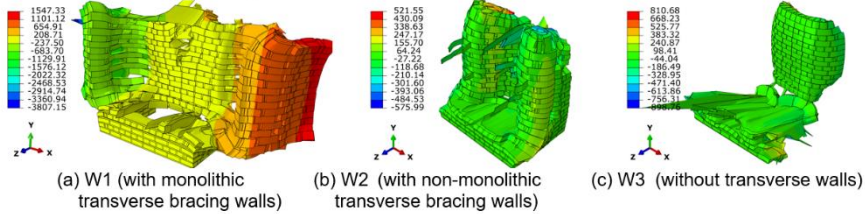


Fig. 8. X-displacement (mm) distributions

Scaled distance: $2.19\text{m/kg}^{1/3}$

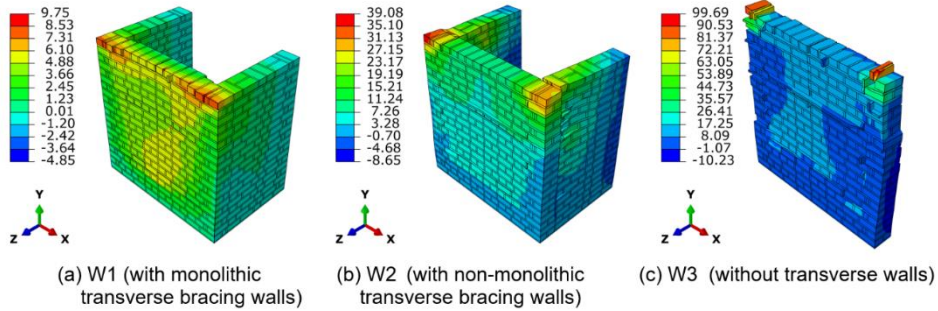
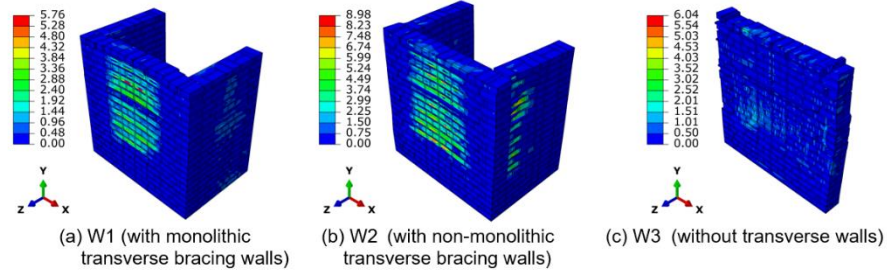


Fig. 9. Y-displacement (mm) distributions at $2.19\text{m/kg}^{1/3}$

Scaled distance: $2.19\text{m/kg}^{1/3}$



Scaled distance: $1.83\text{m/kg}^{1/3}$

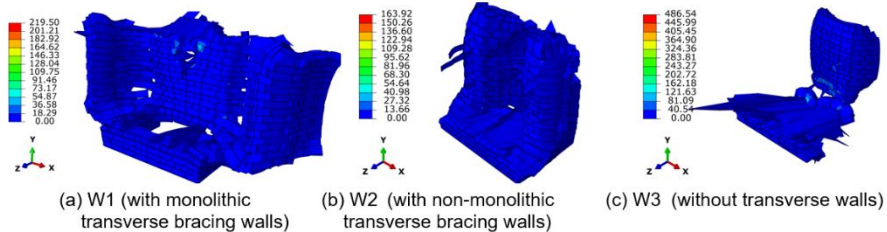


Fig. 10. Shear stress (MPa) distributions: I

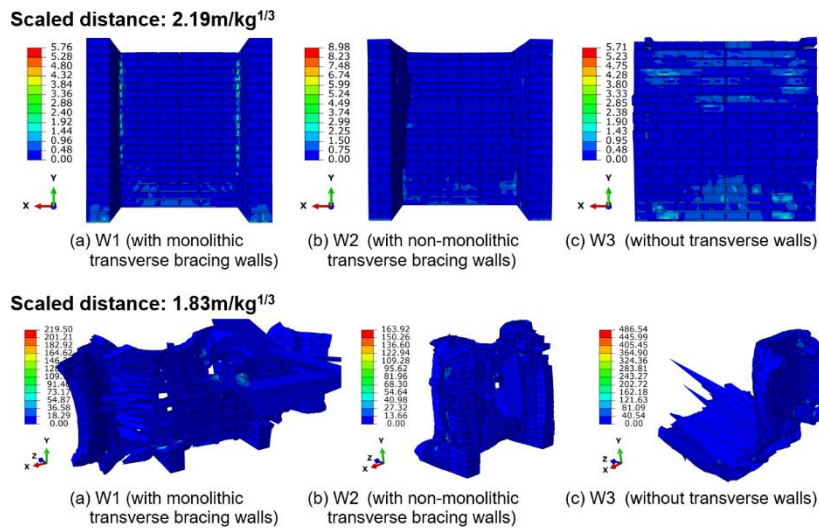


Fig. 11. Shear stress (MPa) distributions: II

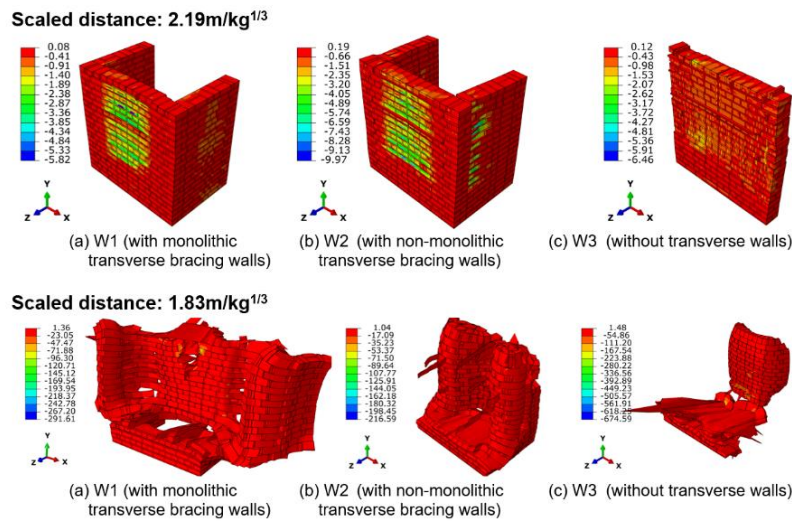


Fig. 12. Principal stresses (MPa) distributions: I

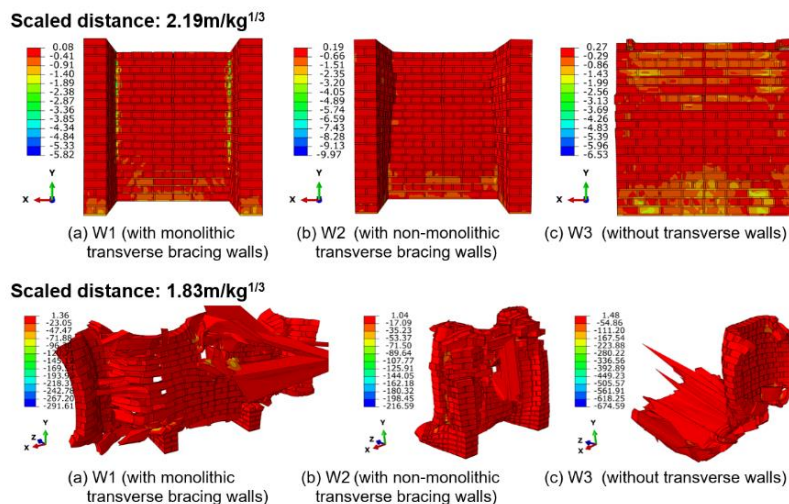


Fig. 13. Principal stresses (MPa) distributions: II

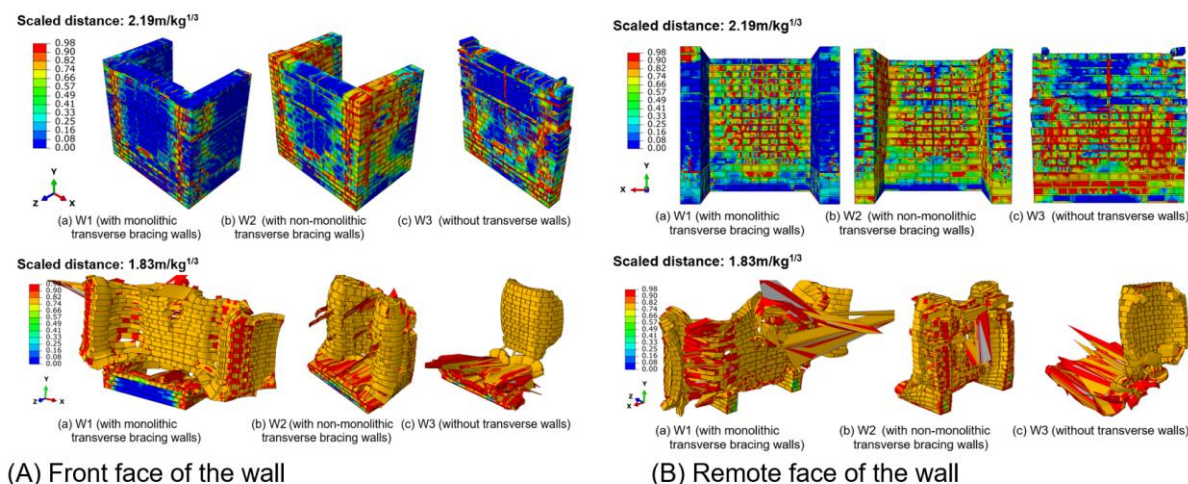


Fig. 14. Damage patterns

Table 1. Summary of responses: Part I

| Wall | Δ_{max} (mm) | | Maxm. DDE (J) | |
|------|--------------------------|-----------|---------------------------|-----------------------------|
| | Z=2.19 | Z=1.83 | Z=2.19 | Z=1.83 |
| *W1 | 58.34 | >>>>230 | 336.78 | 14033.70 |
| #W2 | 65.62 (^a 9) | >>>>>230 | 420.98 (^a 25) | 15998.42 (^a 14) |
| ##W3 | 71.66 (^a 23) | >>>>>>230 | 390.66 (^a 16) | 17401.80 (^a 24) |

* is braced URM wall with monolithic transverse bracing walls; # is URM wall with non-monolithic transverse bracing walls; and ## is free-standing wall (without transverse walls); Δ_{max} : maximum transverse permanent displacement of the out-of-plane exposed braced wall; DDE: damage dissipation energy; ^a percentage increase with respect to wall W1

Table 2. Summary of responses for exposed wall: Part II

| Wall | Maxm. shear stress (MPa) | | principal stress (MPa) | |
|------|---------------------------|-----------------------------|-------------------------|------------------------------|
| | Z=2.19 | Z=1.83 | Z=2.19 | Z=1.83 |
| W1 | 2.88 | 18.29 | 3.36 | 23.05 |
| W2 | 7.48 (^a >100) | 27.32 (^a 49) | 5.74 (^a 71) | 35.23 (^a 53) |
| W3 | 3.52 (^a 22) | 81.09 (^a >>100) | 3.72 (^a 11) | 111.20 (^a >>100) |

^a percentage increase with respect to wall W1

Predicting the structural response to a specific blast level is crucial for ensuring its safety. Load-bearing masonry structures, such as culverts, bridges, monuments, and palaces, commonly employ bracing walls. These walls can be either monolithic or non-monolithic, with the main wall. A monolithic joint between the walls restricts both rotational and transverse displacements of the braced wall, while a non-monolithic connection only restrains transverse displacement. The presence of two joints between the walls causes the exposed wall to respond differently to blast loads, thereby influencing the resulting damage. Hence, it is crucial to comprehend the response of walls featuring these joints when subjected to explosive forces.

2. Objectives and Methodology

This research study represents the pioneering numerical analysis of two types of braced walls: those with monolithic transverse bracing walls and those with non-monolithic transverse bracing walls. Additionally, it investigates the performance of free-standing walls (without transverse walls) when subjected to close-in explosion loading at 2.19 and 1.83m/kg^{1/3}. The study examines the impact of both monolithic and non-monolithic transverse bracing walls on the out-of-plane exposed wall. Moreover, it highlights the significance of the monolithic connection between the exposed wall and transverse walls. The findings of this research shed light on the extent of damage to URM walls and propose constructional enhancements to mitigate the effects of blast loading on masonry walls. This paper's scope encompasses various structures, including historic masonry monuments of national and international significance, as well as parliament buildings, courts, and nuclear containments.

The examination of various methodologies for analyzing the behavior of masonry walls under different blast loading scenarios has captivated the interest of many academics. A vast majority of researchers employ the widely-used

numerical technique known as the FEM to evaluate structures under diverse dynamic loading conditions, such as blast, impact, and wind. Consequently, presented below are the FEM investigations conducted by the research team.

3. Literature Review

- **Blast load mechanism**

Explosions in Beirut, Lebanon, have highlighted the importance of blast-resistant design not only for high-profile structures like embassies and military institutions but also for buildings in general [13, 15–17]. The devastating blast in Beirut resulted in over 200 confirmed fatalities and more than 6,000 people injured. The estimated cost of infrastructure damage is between \$10 and \$15 billion. The safety of buildings in the face of explosive forces has become a major concern for structural engineers. The collapse of nearby structures and the damage inflicted on distant buildings has heightened these worries. In Ryazan, Russia, there is currently a constant bombardment of artillery shells occurring every ten seconds. This is the result of an accidental explosion caused by a sweeping glaze that ignited an ammunition storage facility nearby [8]. The evacuation of over 2,300 residents was necessary within a 5-kilometer radius of the ammunition depot. Based on gathered data, the potential impact of the explosion on the affected structures could vary from repairable damage to complete collapse, resulting in fatalities [2, 9–17]. A team of engineers strongly advocates for the implementation of designs that can withstand such intense forces in areas prone to vulnerability or conflict, emphasizing the importance of preserving human safety and the structural integrity of buildings [13].

To generate any form of explosion that goes beyond mere fire, it is necessary to utilize chemical explosives that are solid and uncovered [13, 15, 17]. This process is known as detonation, wherein the non-reactive explosive material undergoes a rapid and solid chemical reaction [26–28]. The velocity of detonation is measured within the range of $6e+3$ to $8e+3$ m/s [26–27]. Whether in solid or liquid form, the explosive transforms into a dense, intensely hot gas under extreme pressure. The detonation of a significant quantity of explosive material creates shockwaves that consist of a high-intensity pressure front, expanding outward into the surrounding atmosphere [26–28]. Due to the dispersion of air in a spherical pattern, there is a correlation between the decrease in blast pressure and an increase in the duration of the blast wave, resulting in a decrease in velocity [26]. As the pressure front expands and propagates, it encounters and engulfs any obstacles in its path, subjecting the entire building to blast pressures [26–28]. The time it takes for the blast wave to reach a specific location, known as the time of arrival (t_a), can be observed through Friedlander's blast pressure time history depicted in [25]. When the incident pressure reaches its peak, there is an immediate increase in air pressure (P_s). The blast pressure profile can be separated into two distinct phases: a positive phase, which endures for a period of time known as t_s , in which the pressure exceeds that of the surrounding atmosphere, and a negative phase, which lasts for t_s^- and is characterized by a pressure lower than atmospheric. It is within the area below the blast pressure profile that the blast impulse takes place.

The peak value of the blast pressure front is influenced by two key factors: explosive mass and scaled distance [8–13]. These factors play a significant role in determining the intensity of the blast.

- **Overview of past studies**

There are numerous simulations based on finite element analysis that can be accessed in the public domain, which have extensively examined the behavior of brick masonry URM walls. Additionally, a multitude of experimental studies have also been conducted on this subject. In the work cited as [29] and [30], the influence of support conditions and wall thickness on the URM wall's ability to withstand blast loading was investigated. Researchers [31], [24], [22], and [23] identified that increasing the wall thickness enhances its resistance against blast effects. Furthermore, [31] undertook a numerical study to assess the impact of brick and mortar strength on the URM wall's response to low-intensity blast loading. The study concluded that higher strength in both the brick unit and joint mortar resulted in reduced maximum deflection and support rotation. These findings underscore the significance of comprehending the structural elements of URM walls and their behavior during blast events. In a study conducted by [22], it was discovered that as the compressive strength of the masonry increased, there was a decrease in the maximum deflection of the infill masonry walls. Similarly, [31] and [30] reported that the response of the wall mainly depended on its specific support. [10], in their experimental study, observed no significant damage to the free-standing clay brick URM wall at a scaled distance of $2.28 \text{ m/kg}^{1/3}$ (peak pressure=0.21MPa). [20] conducted a numerical study using LS-DYNA software and reported a complete collapse of the infill CMU masonry wall of an RC frame structure at a scaled distance of $2.37 \text{ m/kg}^{1/3}$. The mode of damage and fragmentation of the wall into debris, as well as their expulsion, were primarily influenced by blast reflected pressure, impulse, and wall thickness [32]. The response of a target structure to a specific type of loading is influenced by several key factors. The determination of these variables encompasses multiple factors, such as the specific attributes of the blast load wave, the structural configuration, the type of support provided, the dynamic characteristics of the material composition, and the inherent natural frequency of the target structure. This valuable insight is derived from reference [33].

Experiments were carried out by [34] to explore the effects of strain rate on the characteristics of brick and mortar materials through dynamic uniaxial compression. The findings demonstrated a substantial enhancement in the compressive strength of both brick and mortar as the strain rate increased. In another study, [35] proposed a methodology for assessing the structural reliability of conventional masonry walls under vertical bending conditions. The results revealed that the reliability of these structures is significantly influenced by various factors, including wall width, quality of workmanship, and the discretization of masonry unit thickness. Furthermore, a method was introduced by [36] to evaluate the dependability of masonry walls when exposed to explosive forces. This methodology integrates analytical reliability techniques with nonlinear finite element analysis. The research highlighted that the most influential random variables affecting the resistance of masonry walls are the strength of mortar joints and the friction between contact surfaces.

In their research, [37] utilized LS-DYNA software to simulate the reactions of a clay brick masonry wall reinforced with different types of fiber-reinforced polymers (FRPs). The purpose was to investigate the effectiveness of FRP strengthening in withstanding blast loads. In a similar manner, [38] utilized AUTODYN software in conjunction with custom subroutines to establish the distinct characteristics of clay bricks and mortar. Their objective was to anticipate the reaction and degradation of a masonry wall when exposed to explosive forces. One strategy for reducing computational requirements is to employ a homogenized masonry material model. The determination of the equivalent elastic moduli for brick masonry was carried out by [39] through the examination of the elastic properties of its individual components. On the other hand, [40] presumed that masonry material behaves as an orthotropic substance with both elastic and brittle characteristics, and then derived its homogenized mechanical properties. In [41], numerical methods were employed to calculate the global elastic coefficients of masonry, considering the finite thickness of the structure. Thorough research and analysis play a vital role in comprehending the behavior and reaction of masonry structures to blast loads, as emphasized by these studies.

- **Available strategies to model masonry in Abaqus**

In the realm of masonry numerical representation, there are two primary approaches: micro-modeling and macro-modeling. Micro-modeling involves individually representing the various components of masonry, such as bricks, blocks, and mortar. On the other hand, macro-modeling treats masonry as a composite entity. The choice between these approaches depends on the required level of precision and simplicity. Macro-modeling entails blending the units, mortar, and their interactions into a homogenous continuum. This approach is suitable for cases where a broad overview is sufficient. Alternatively, simplified micro-modeling groups together the behavior of mortar joints and unit-mortar interfaces using dis-continuum elements, while representing enlarged units with continuum elements. For a more detailed analysis, detailed micro-modeling becomes necessary. This approach utilizes continuum elements to represent the units and mortar in the joints, while dis-continuum elements are employed to depict the unit-mortar interface. Figure 1 presents a graphical depiction of the various strategies employed in modeling. The selection of a modeling approach is contingent upon the accessibility and dependability of data, the desired degree of precision, and the desired level of simplicity [42]. Macro-modeling is the most realistic finite element technique, as it requires less memory and computational time. Achieving a harmonious equilibrium between precision and effectiveness proves beneficial. On the other hand, micro-models require significant processing power to achieve the highest level of precision [42].

This work utilizes a meticulous approach to micro-modeling, which eliminates the unit-joint interface and instead assumes a flawless bond through merged interface nodes. The following subsection delves extensively into the intricacies of micro-modeling in brickwork.

- **Micro-modeling**

Extensive investigation has been carried out in the public domain regarding the micro-modeling of masonry. Numerous research endeavors, such as the works of [43-49], delve into this subject matter. In the micro-modeling technique, building blocks (such as bricks, stones, or blocks) and joint mortar are treated as distinct components of the wall. Furthermore, special attention is given to the mortar interface. When bricks and mortar joints slide at these interfaces, the limited cohesion between the brick unit and joint mortar is activated [50]. The current investigation employs models for friction, hard contact, cohesion, and damage evolution to conduct a comprehensive analysis of the interaction between the brick unit and mortar joint. The adhesion of materials is affected by the shear and normal stresses encountered at the surfaces of the masonry joint. This failure criterion for the interface between the brick unit and mortar joint is expressed by Equation (1) [8, 22-23].

$$\left(\frac{|\sigma_N|}{\sigma_{Nmax}}\right)^2 + \left(\frac{|\sigma_S|}{\sigma_{Smax}}\right)^2 + \left(\frac{|\sigma_T|}{\sigma_{Tmax}}\right)^2 = 1 \quad \text{Eq. (1)}$$

Here, σ_N = normal stress; σ_N^{max} = tensile strength; σ_s = tangential shear; σ_s^{max} = shear strength; σ_T = tangential shear; σ_T^{max} = shear strength (MPa).

4. Numerical modeling

Abaqus/Explicit, a commercial software, is employed to conduct a numerical analysis through the finite element method. This software has been effectively utilized in scenarios with similar loading conditions [8-13] and comparable materials [22-23, 40]. The numerical modeling tool Abaqus/Explicit offers the capability to simulate blast loading using the ConWep blast load calculation module, which employs semi-empirical techniques. However, the detonation process of the explosion, the propagation of the blast wave through the air, and its impact with the wall cannot be accurately modeled when employing the semi-empirical algorithm for blast load calculation. Despite its limitations, the semi-empirical code has demonstrated its ability to generate blast loads that are deemed satisfactory in comparison to computationally intensive programs based on computational fluid dynamics [13, 25].

- **FE information**

Three FE models have been developed using a comprehensive micro-modelling approach, as illustrated in Figure 2. The initial model, referred to as W1, features a 230mm thick unreinforced brick masonry wall that is reinforced with monolithic transverse walls. These transverse walls are constructed using solid clay bricks with dimensions of 230mm x 110mm x 71mm. The experimental testing of this model was conducted by [33], as shown in Figure 2(a). The mortar joints in this model have a thickness of 20mm, which may be considered relatively high. However, for consistency with the experimental study conducted by [33], the present study also utilized 20mm thick mortar joints. The bricks in this model are arranged in a running bond configuration. The second model, denoted as W2, involves introducing a non-monolithic connection between the supporting transverse walls and the braced exposed wall of the first model, as depicted in Figure 2(b). This modification allows for the examination of the structural behavior when the connection between the transverse walls and the exposed wall is not monolithic. Lastly, the third model, known as W3, represents the exposed wall of either model W1 or W2 without any transverse supports. This model is designed to simulate a free-standing wall scenario, as illustrated in Figure 2(c).

The C3D8R element is used to discretize the brick unit and joint mortar [52, 8-13], ensuring a detailed and accurate final mesh. After conducting a mesh sensitivity test at a scaled distance of 2.19m/kg^{1/3}, a mesh size of 10mm is determined to be appropriate, as it prevents convergence issues and yields accurate results. In order to accurately depict the connection between the brick units and mortar joints, the numerical model necessitates incorporating interactions and constraint conditions. It is crucial to establish a strong connection between the continuum finite elements of the mortar joints and those of the brick units. Consequently, the nodes are combined, and the bond interface between the brick and mortar is not explicitly defined. By default, the program employs contact enforcement with a penalty stiffness ten times greater than that of the underlying element. This ensures proper adherence and stability within the model. A detailed mesh is created to ensure accuracy, with a mesh size of 10mm determined through sensitivity testing. The numerical model incorporates interactions and constraint conditions to accurately represent the contact relationship. The default contact enforcement establishes a strong bond between the brick and mortar components, maintaining stability throughout the analysis.

To ensure proper response to external forces, it is essential for masonry walls to have appropriate boundary conditions. These walls are supported by a fixed surface, typically the ground. In order to simulate this ground in the program being utilized, the REFERENCE POINT command is employed [8, 52]. Consequently, the numerical models are limited by the reference experimental tests conducted by [33]. The relationship between the wall and any given surface is established through contact interaction, utilizing contact models along with the penalty contact approach as a mechanical constraint formulation.

It is important to highlight that the cohesive behavior is characterized by the traction-separation relationships that are included as default in Abaqus [57-58]. The friction coefficient assigned to the brick-to-mortar contact is set at 0.75. Additionally, it is crucial to acknowledge the significance of roller supports positioned on the bottom face of brick walls from an experimental standpoint. These supports provide the walls with a simply supported condition that is disregarded in numerical models. In order to replicate the effects of a blast, the pressure exerted is represented as a function, using the equivalent mass of TNT and the distance from the explosion site. The LOAD SEGMENT keycard is employed in Abaqus to apply this load, while the explicit solver is used to accurately model the impact of an air-blast on brick walls. The solver in question effectively resolves the motion equation by progressively addressing the problem in small increments. It dynamically adjusts the stiffness matrix following each load and displacement step. Furthermore, it accounts for both geometric and material non-linearity, ensuring a comprehensive analysis of the system's behavior [52].

The CONWEP code offers users a means to apply load on a structure by providing peak pressure and impulse values. In the case of the exposed out-of-plane braced wall, experimental blast reflected peak pressures of 0.38 and 1.01MPa were observed. These pressures were generated from explosive charges with scaled distances of 2.19 and 1.83m/kg^{1/3} in free air, weighing 4.34 and 7.49kg-TNT equivalent, respectively. The burst occurred at a height of 910mm above the ground surface, as depicted in Figure 3 which illustrates the location of the explosive charge. Figure 4(a) presents an idealized profile proposed by [53], based on chemical explosions. Air-blast loading characteristics and related blast parameters are thoroughly discussed by the authors in Refs [9-13]. Additionally, Figure 4(b) showcases free-air blast shockwave profiles recorded experimentally by [33].

5. Results

• Verification of the Numerical Model (W1)

For $Z=2.19\text{m/kg}^{1/3}$ ($t=137\text{ms}$): On the surface affected by the explosion, the wall that was exposed has experienced two types of cracks. Firstly, there are vertical cracks located at the middle part of the wall that extend throughout its entire thickness. These cracks are caused by rotation and are also present near the joints where the wall connects with the monolithic bracing transverse walls. In addition, there exist cracks running parallel to the ground at the lower level. The illustration in Figure 5 displays the fringe levels that serve as indicators of the wall's damage severity. A fringe level of 0.0 signifies no damage, whereas a level of 0.98 signifies substantial damage, resulting in a notable decrease in the masonry's strength and rigidity. As for the material itself, softening behavior begins when the fringe level reaches approximately 0.49. Furthermore, there is a significant issue with the connection between the mortar and brick in the uppermost layer, causing a substantial transverse displacement of 70.28mm. In addition, vertical cracks have appeared in the supporting walls where the upper portion of the wall widens. These cracks extend down to the sixth course and taper off as they progress, as shown in Figure 5. Additionally, diagonal cracks have appeared in the transverse walls near the ground. On the back face of the exposed wall, numerous vertical cracks with greater width at the top have formed, reaching almost halfway up the wall, as depicted in Figure 5. The wall system has experienced significant damage, measured as a DDE (Damage Degree Equivalent) of 336.78J, and a maximum transverse permanent displacement of 58.34mm at the midpoint of the exposed wall near its upper section, as outlined in Table 1. It is important to note that the workmanship and construction quality of the tested walls, as examined by [33], raise concerns and may explain their poor performance. These damages observed in the URM braced wall align closely with the findings reported by Ref. [33] in their experimental study, as illustrated in Figure 5 to Figure 7.

Monolithic transverse walls serve as shear walls, offering structural support for the exposed masonry braced wall. As a result of the blast, these walls experience both in-plane and transverse displacements. The average maximum in-plane displacement is measured at 10.57mm, while the average maximum transverse displacement is recorded at 12.33mm (refer to Figure 8 and Figure 9). Furthermore, the masonry braced wall that is exposed experiences upward displacement, with the most significant displacement observed at the center of the wall and gradually decreasing towards the junctions of the wall (refer to Figure 10). This is due to the cohesive nature of the two walls at the intersection. The occurrence of localized shear failure is identified by the presence of a peak shear stress of 2.88MPa, which is observed at the midpoint of the interface between the mortar and brick in the stretcher course of the upper two-thirds section of the exposed braced wall. In contrast, the transverse walls undergo a peak shear stress of 1.44MPa at the central point of their mid-height level. These findings are presented in Table 2 and Figure 10. Additionally, on the backside, the exposed wall encounters a maximum shear stress of 2.88MPa at its junctions with the bracing walls, as depicted in Figure 11. The stress distribution on the front and back surfaces of the exposed wall can be observed in Figure 12 and Figure 13, respectively. IS 1905 [54] and SP 20 [55] have set limitations on the maximum allowable values of compressive, tensile, and shear stresses for brick masonry structures, which are 1.10 MPa, 0.07 MPa, and 0.50 MPa, respectively. On the other hand, the AS 3700 has specified maximum limits of 0.20 MPa for tensile stress and 0.35 MPa for shear stress [56].

For $Z=1.83\text{m/kg}^{1/3}$ ($t=152\text{ms}$): The three walls experience a catastrophic collapse, with significant displacement (equal to or greater than 230mm, which is the thickness of the walls) in their horizontal directions. This collapse is caused by the peak pressure from the blast, which reflects and reaches 1.01MPa, at a scaled distance of 1.83m/kg^{1/3} (as shown in Figure 7). Despite this collapse, a few courses of the bottom part of the walls manage to survive due to the forces of gravity and friction. However, the push exerted on these walls by the blast loading, combined with the reactive thrust from the far ends of the bracing wall, causes the walls to respond by opening outward, ultimately leading to their collapse.

• Performance of wall W2

For $Z=2.19\text{m/kg}^{1/3}$ ($t=137\text{ms}$): Wide vertical cracks have been observed near the upper portion of the visible wall along the supported edges, extending up to the 6th course on the side facing the explosion. Furthermore, a few cracks

have also extended towards the lower part of the wall (Figure 14(b)). On the rear side of the visible wall (W2), a prominent and wide vertical crack has been identified at the mid-span, accompanied by additional vertical cracks on either side. These cracks are further compounded by horizontal cracks in successive layers of mortar at mid-height of the wall (Figure 14). The non-monolithic transverse walls also exhibit vertical cracks near their supporting vertical edges (Figure 14). Upon comparing the damage sustained by wall W2 with that of wall W1 under the same blast loading conditions (0.38MPa), it is evident that the exposed wall W2 and its non-monolithic bracing walls have suffered more severe damage than wall W1 (Figure 14).

The severity of the damage to the bracing walls is reflected in the non-monolithic character of the walls. The response of the exposed wall governs this, resulting in an increase of 9% and 25% in the maximum transverse displacement and damage (DDE) of the non-monolithic wall system (W2) compared to the monolithic wall system (W1), as shown in Table 1. In the non-monolithic bracing walls, the average maximum in-plane and transverse displacements become significant, measuring 37.34mm and 95.97mm respectively, compared to 10.57mm and 12.33mm in the monolithic bracing walls, as depicted in Figure 7 and Figure 8. The transverse walls' top three courses, near the supporting edges, experience a significant upheaval with a maximum displacement of 23.17mm, as shown in Figure 9. The exposed wall of wall system W2 exhibits large transverse displacement and end rotation, causing an eccentric push on the non-monolithic transverse walls. This, in turn, results in substantial out-of-plane inward displacements and ultimately leads to the collapse of the top courses of the transverse walls near the supporting vertical edges, as depicted in Figure 7. The brick-mortar interface of the exposed wall and its non-monolithic buttressing transverse walls (W2) experiences higher Von-mises shear and principal compressive stresses compared to the stresses in wall system W1, as illustrated in Table 2 and Figure 10 to Figure 13.

For $Z=1.83\text{m/kg}^{1/3}$ ($t=152\text{ms}$): The non-monolithic wall system W2, including the exposed masonry wall and transverse walls, experienced significant transverse displacement, ultimately resulting in a complete collapse due to the reflected peak pressure of 1.01MPa at $1.83\text{m/kg}^{1/3}$. This can be observed in Figure 7 and Table 1. The sudden and substantial displacement, coupled with rotation along the vertical ends and an eccentric push, caused the transverse walls to inwardly displace to a large extent, leading to their near simultaneous collapse as depicted in Figure 14.

• Performance of wall W3

For $Z=2.19\text{m/kg}^{1/3}$ ($t=137\text{ms}$): On the surface where the explosion occurred, there are wide cracks that run through the thickness of the wall, specifically along the vertical mortar joints in the middle, near the middle height, and near the edges of the wall. The presence of these cracks is clearly visible in Figure 14. Furthermore, there are also flexure cracks observed along the horizontal mortar joints located at the lower part of the wall. Shear failure happens at the interface between the stretcher course and the horizontal joint mortar near the middle height level, as shown in Figure 14. On the opposite side of the wall, there are horizontal cracks located in the middle of about three-fourths of the wall's length, appearing in the mid-height region (Figure 14). The bricks at the top corners and the adjacent bricks of the topmost layer become almost completely detached due to the failure of the joint mortar. This leads to a significant upward displacement of 99.69mm and a transverse displacement of 81.19mm, as observed in Figure 9 and Figure 7. The free-standing Wall W3 is subjected to significant damage when exposed to the same reflected blast pressure of 0.38MPa, as illustrated in Figure 14. On the other hand, the damage observed in Wall system W1 is less severe due to its monolithic nature and the presence of transverse bracing walls, as shown in Figure 14. Although the exposed wall of W2 experiences more damage compared to W1, it still does not reach the level of damage sustained by the free-standing Wall W3, as depicted in Figure 14. The exposed wall of W3 exhibits a 23% increase in maximum transverse displacement and a 16% increase in damage (DDE) compared to the monolithic wall system, W1, as shown in Table 1. Additionally, the displacement of the exposed wall, W3, is found to be 23% higher than that of W2, as indicated in Table 1. This can be attributed to the damage incurred by the non-monolithic transverse bracing walls. Table 2 and Figure 10 emphasize the occurrence of the highest Von-mises shear stress, measuring 3.52MPa. This stress is found at the interface between the vertical joint mortar and brick, specifically near the mid-height region and at the middle of wall W3.

For $Z=1.83\text{m/kg}^{1/3}$ ($t=152\text{ms}$): In the event of a significant horizontal displacement occurring in the joint mortar layer near the base of a free-standing exposed wall, there is a high risk of the wall collapsing entirely. This can be observed in Table 1 and Figure 14.

6. Conclusions

In this study, a highly detailed three-dimensional micro-model of a clay brick masonry wall, reinforced with two solid transverse bracing walls (referred to as W1), one on each end, has been created using the Abaqus commercial software. The main goal of this study is to examine how the wall reacts when exposed to blast loads that are directed away from its plane. To accomplish this, a plasticity-based constitutive model for masonry and an explicit solver for blast

simulations, both available in the Abaqus code, have been utilized. The results obtained from the software simulations closely align with the experimental findings conducted by [33]. This validation process ensures the accuracy and reliability of the developed model. With the validated model in place, the study delves into two primary investigations: (i) analyzing the impact of monolithic and non-monolithic transverse bracing walls on the performance of the exposed wall under out-of-plane blast loads, and (ii) assessing the significance of the monolithic connection between the exposed wall and transverse walls. To address these objectives, two additional wall models have been created: (1) W2, which represents an exposed braced wall with non-monolithic transverse bracing walls, and (2) W3, a free-standing exposed wall without any transverse walls. Through comprehensive analysis and comparison of these different models, several conclusions have been drawn.

- The level of damage in wall system W1 is relatively less severe (DDE=336.78J) due to the presence of monolith joints and transverse bracing walls. On the other hand, the exposed wall of W2 has experienced greater damage with a DDE of 420.98J compared to the exposed wall of W1, but it is still not as severe as the damage observed in the free-standing wall W3 (DDE=390.66J).
- The existence of non-monolithic connections between the visible wall and the transverse bracing walls suggests a higher probability of damage to the bracing walls. This damage is primarily influenced by the response of the exposed wall. Therefore, it is crucial to prioritize strengthening the exposed out-of-plane masonry wall in order to mitigate the potential threat posed by explosions. This approach allows for a more effective safeguarding of the overall structure.
- To mitigate the risk of significant injuries and casualties caused by large displacements at the top courses of brick walls, it is crucial to implement appropriate strengthening techniques. The presence of weak mortar and the free-boundary condition contribute to material loss and potential structural failure. To address this issue, reinforcing the wall with concrete bands or introducing pre-compression can effectively restrain displacements and control damage. By employing these measures, the structural integrity of the wall can be enhanced, reducing the likelihood of dangerous incidents.
- The connections where exposed and bracing walls meet experience a more intricate stress condition, making them crucial for managing overall damage caused by blast loading. To mitigate failure, it is necessary to enhance the ductility of these wall junctions by incorporating specific forms of reinforcement on the wall surfaces.
- In the realm of masonry structures, the effectiveness and caliber of construction hold utmost significance when it comes to their ability to withstand blast loading.

References

1. Myers J J, Belarbi A, and El-Domiati A K (2004), "Blast resistance of FRP retrofitted un-reinforced masonry (URM) walls with and without arching action", *TMS Journal*, pp. 9-26.
2. Anas S M, Ansari Md I, and Alam M (2020), "Performance of masonry heritage building under air-blast pressure without and with ground shock", *Australian Journal of Structural Engineering*, 21(4): 329-344, <https://doi.org/10.1080/13287982.2020.1842581>.
3. Padalu R V K P, Singh Y, and Das S (2020), "Analytical modelling of out-of-plane flexural response of unreinforced and strengthened masonry walls", *Engineering Structures*, vol. 218. <https://doi.org/10.1016/j.engstruct.2020.110797>.
4. Gad F. E., Wilson L. J., Moore J. A., Richards B. A. 2005, "Effects of mine blasting on residential structures", *Journal of Performance of Constructed Facilities*, ASCE, Vol. 19, No. 3, pp. 222-228. [https://doi.org/10.1061/\(ASCE\)0887-3828\(2005\)19:3\(222\)](https://doi.org/10.1061/(ASCE)0887-3828(2005)19:3(222)).
5. Heath J. D., Wilson L. J., and Gad F. E. 2015, "Acceleration-displacement response spectrum vibration limits for blast vibrations", *Australian Journal of Structural Engineering*, Taylor & Francis, Vol. 16, No. 1, pp. 1-16. DOI: 10.7158/13287982.2015.11465175.
6. Moore J. A., Richards B. A., Gad F. E., and Wilson L. J. 2003, "Structural response of brick veneer houses to blast vibration", *Proceedings of the 29th Annual Conference on Explosives and Blasting Technique*, Nashville, Tennessee, U.S., Vol. 2, pp. 223-230.
7. Tsang H. H., Gad F. E., Wilson L. J., Jordan W. J., Moore J. A., and Richards B. A. 2017, "Mine blast vibration response spectrum for structural vulnerability assessment: case study of heritage masonry buildings",

- International Journal of Architectural Heritage: Conservation, Analysis, and Restoration*, Taylor & Francis, Vol. 12, No. 2, pp. 270-279.
8. Anas S M and Alam M (2021), "Air-Blast Response of Free-Standing: (1) Unreinforced Brick Masonry Wall, (2) Cavity RC Wall, (3) RC Walls with (i) Bricks, (ii) Sand, in the cavity: A Macro-Modeling Approach", *In: Marano G.C., Ray Chaudhuri S., Unni Kartha G., Kavitha P.E., Prasad R., Achison R.J. (eds) Proceedings of SECON'21. SECON 2021. Lecture Notes in Civil Engineering*, volume 171. Springer, Cham, pp. 921-930. https://doi.org/10.1007/978-981-33-6389-2_18.
 9. Anas S M, Ansari Md I, and Alam M (2021), "A study on existing masonry heritage building to explosive-induced blast loading and its response", *International Journal of Structural Engineering*, 11(4): 387-412, doi/abs/10.1504/IJSTRUCTE.2021.118065.
 10. Ahmad S, Elahi A, Pervaiz H, Rahman A, and Barbhuiya S (2013), "Experimental study of masonry wall exposed to blast loading", *Mater. Construcción*, 64(313), pp. 1-11.
 11. Anas S M, Alam M, and Umair M (2021), "Experimental and Numerical Investigations on Performance of Reinforced Concrete Slabs under Explosive-induced Air-blast Loading: A state-of-the-art review", *Structures*, Elsevier, 31: 428-461, <https://doi.org/10.1016/j.istruc.2021.01.102>.
 12. Anas S M, Alam M, and Umair M (2021), "Air-blast and ground shockwave parameters, shallow underground blasting, on the ground and buried shallow underground blast-resistant shelters: A review", *International Journal of Protective Structures*, 13(1): 99-139, <https://doi.org/10.1177/2F20414196211048910>.
 13. Anas S M, Alam M, and Shariq M (2022), "Damage Response of Conventionally Reinforced Two-way Spanning Concrete Slab under Eccentric Impacting Drop Weight Loading", *Defence Technology*, <https://doi.org/10.1016/j.dt.2022.04.011>.
 14. Abdullah F K, Cunningham S L, and Gillie M (2017), "Simulating masonry wall behavior using a simplified micro-model approach", *Engineering Structures*, vol. 151, pp. 349-365. <https://doi.org/10.1016/j.engstruct.2017.08.021>.
 15. Valente M and Milani G (2016), "Non-linear dynamic and static analyses on eight historical masonry towers in the north-east of Italy" *Engineering Structures*, 114(1), pp. 241-270. <https://doi.org/10.1016/j.engstruct.2016.02.004>.
 16. Valente M and Milani G (2016), "Seismic assessment of historical masonry towers by means of simplified approaches and standard FEM" *Construction and Building Materials*, 108(1), pp. 74-104. <https://doi.org/10.1016/j.conbuildmat.2016.01.025>.
 17. Drougkas A, Licciardello L, Rots J G, and Esposito R (2020), "In-plane seismic behaviour of retrofitted masonry walls subjected to subsidence-induced damage", *Engineering Structures*, vol. 223, <https://doi.org/10.1016/j.engstruct.2020.111192>.
 18. Penna A, Morandi P, Rota M, Manzini C F, Da Porto F, and Magenes G (2013), "Performance of masonry buildings during the Emilia 2012 earthquake", *Bull Earthq Eng*, 12. <https://doi.org/10.1007/s10518-013-9496-6>.
 19. Padalu P K V R, Singh Y, and Das S (2020), "Analytical modelling of out-of-plane flexural response of unreinforced and strengthened masonry walls", *Engineering Structures*, vol. 218, <https://doi.org/10.1016/j.engstruct.2020.110797>.
 20. Wu C and Hao H (2007), "Safe scaled distance for masonry infilled RC frame structures subjected to airblast loads", *Journal of Performance of Constructed Facilities*, ASCE, 21(6), pp. 422-431. [https://doi.org/10.1061/\(ASCE\)0887-3828\(2007\)21:6\(422\)](https://doi.org/10.1061/(ASCE)0887-3828(2007)21:6(422)).
 21. Yu J, Gan P Y, Wu J, and Wu H (2019), "Effect of concrete masonry infill walls on progressive collapse performance of reinforced concrete infilled frames", *Engineering Structures*, vol. 191, pp. 179- 193. <https://doi.org/10.1016/j.engstruct.2019.04.048>.
 22. Pereira J M, Campos J, and Lourenço P B (2014), "Experimental study on masonry infill walls under blast loading", *In: Proceedings of the 9th International Masonry Conference*, pp. 1-9.
 23. Parisi F, Balestrieri C and Asprone D (2016), "Out-of-plane blast capacity of load-bearing masonry walls", *16th International Brick & Block Masonry Conference*, Padova, Italy, pp. 991-998.
 24. Pandey A and Bisht R (2014), "Numerical modelling of infilled clay brick masonry under blast loading", *Advances in Structural Engineering*, 17(4), pp. 591-606. <https://doi.org/10.1260/2F1369-4332.17.4.591>.
 25. Hao H, Hao Y, Li J, and Chen W (2016), "Review of the current practices in blast-resistant analysis and design of concrete structures", *Advances in Structural Engineering*, SAGE, 19(8): 1193-1223. <https://doi.org/10.1177/2F1369433216656430>.
 26. TM 5-1300(1990), "Structures to resist the effects of accidental explosions", TM 5-1300, Joint Department of the Army, the Navy and the Air Force Technical Manual, Department of Defence Explosives Safety Board, Alexandria, Virginia.

27. UFC 3-340-02 (2008), "Structures to resist the effects of accidental explosions", Unified Facilities Criteria UFC 3-340-02, U.S. Army Corporations of Engineers.
28. TM 5-855-1 (1986), "Design & analysis of hardened structures to conventional weapons effects", TM 5-855-1, U.S. Department of the Army.
29. Knox K J, Hammons M I, Lewis T T, and Porter J R (2000), "Polymer materials for structural retrofit, force protection branch, air expeditionary forces technology division, air force research laboratory", Technical Report, Fla, USA: Tyndall AFB, Panama.
30. El-Domiaty K A, Myers J J, Belarbi A (2002), "Blast resistance of un reinforced masonry walls retrofitted with fiber reinforced polymers" In: *Center for infrastructure engineering studies report 02-28*, Rolla, Missouri: University of Missouri.
31. Wei X and Stewart M G (2010), "Model validation and parametric study on the blast response of unreinforced brick masonry walls" *International Journal of Impact Engineering*, 37(11), pp. 1150-1159. <https://doi.org/10.1016/j.ijimpeng.2010.04.003>.
32. Keys R A and Clubley S K (2017), "Experimental analysis of debris distribution of masonry panels subjected to long duration blast loading", *Engineering Structures*, vol. 130, pp. 229-241. <https://doi.org/10.1016/j.engstruct.2016.10.054>.
33. Badshah E, Naseer A, Ashraf M, and Ahmad T (2021), "Response of masonry systems against blast loading", *Defence Technology*, vol. 17, pp. 1326-1337. <https://doi.org/10.1016/j.dt.2020.07.003>.
34. Hao H and Tarasov B (2008), "Experimental study of dynamic material properties of clay brick and mortar at different strain rates", *Australian Journal of Structural Engineering*, vol. 8, pp. 117-131. <https://doi.org/10.1080/13287982.2008.11464992>.
35. Stewart M G and Lawrence S (2002), "Structural Reliability of Masonry Walls in Flexure", *International Journal of Masonry*, 15(2), pp. 48-52.
36. Eamon C D (2007), "Reliability of Concrete Masonry Unit Walls Subjected to Explosive Loads", *Journal of Structural Engineering*, ASCE, Vol. 133, Issue 7, pp. 935-944. [https://doi.org/10.1061/\(ASCE\)0733-9445\(2007\)133:7\(935\)](https://doi.org/10.1061/(ASCE)0733-9445(2007)133:7(935)).
37. Moreland C, Hao H, and Wu C Q (2005), "Response of retrofitted masonry walls to blast loading", *Proceedings of the 6th Asia-Pacific Conference on Shock and Impact Loads on Structures*, Perth, Western Australia, 7-9 December, pp. 405-412.
38. Zhou X Q, Hao H, and Deeks A J (2006), "Numerical modeling of response and damage of masonry walls to blast loading", *Transactions of Tianjin University*, Vol. 12, pp. 132-137.
39. Pande G N, Liang J X, and Middleton J (1989), "Equivalent elastic moduli for brick masonry", *Computers and Geotechniques*, Vol. 8, pp. 243-265.
40. Pietruszczak S and Niu X (1992), "A mathematical description of macroscopic behaviour of brick masonry", *International Journal of Solids and Structures*, Vol. 29, No. 5, pp. 531-546.
41. Anthoine A (1995), "Derivation of the in-plane elastic characteristics of masonry through homogenisation theory", *International Journal of Solids and Structures*, Vol. 32, No. 2, pp. 137-163.
42. Dauda J A, Silva L C, Lourenço P B, and Iuorio O (2021), "Out-of-plane loaded masonry walls retrofitted with oriented strand boards: Numerical analysis and influencing parameters", *Engineering Structures*, vol. 243, <https://doi.org/10.1016/j.engstruct.2021.112683>.
43. Zucchini A and Lourenço P B (2002), "A micro mechanical model for the homogenization of masonry", *International Journal of Solids Structures*, 39(12), pp. 3233-3255.
44. Pina-Henriques J and Lourenço P B (2004), "Masonry micro modeling adopted a discontinuous framework", *Proceedings of the 7th International Conference on Computational Structures Technology*, Lisbon, Portugal.
45. Casolo S (2004), "Modelling in-plane micro-structure of masonry walls by rigid", *International Journal of Solids Structures*, 41(13), pp. 3625-3641.
46. Berto L, Saetta A, Scotta R, and Vitaliani R (2005), "Failure mechanism of masonry prism loaded in axial compression", *Comput. Aspects, Mater. Struct.*, 38(2), pp. 249-256.
47. Chaimoon K and Attard M M (2006), "Modeling of unreinforced masonry walls under shear and compression", *Engineering Structures*, 29(9), pp. 2056-2068. <https://doi.org/10.1016/j.engstruct.2006.10.019>.
48. Milani G, Lourenço P B, and Tralli A (2005a), "A micro mechanical model for the homogenized limit analysis of out-of-plane loaded masonry walls", *Proceedings of the 10th International Conference on Civil, Structural Environmental Engineering Computing*, Rome, Italy.
49. Milani G, Lourenço P B, and Tralli A (2005b), "A simple homogenized micro mechanical model for the analysis at the collapse of out-of-plane loaded masonry walls", *Proceedings of the 17th Congresso AIMETA di Meccanica Teorica e Applicata*, pp. 1-12, Frenze, Italy.

50. Yu J, Gan P Y, Wu J, and Wu H (2019), "Effect of concrete masonry infill walls on progressive collapse performance of reinforced concrete infilled frames", *Engineering Structures*, vol. 191, pp. 179- 193. <https://doi.org/10.1016/j.engstruct.2019.04.048>.
51. Hao H (2009), "Numerical modeling of masonry wall response to blast loads", *Australian Journal of Structural Engineering*, vol. 10, issue no. 1, pp. 37-51. <https://doi.org/10.1080/13287982.2009.11465031>.
52. ABAQUS/Explicit finite element software package (2020), "Concrete Damage Plasticity model, explicit solver, three dimensional solid element library", ABAQUS DS-SIMULIA User Manual, version 6.15.
53. Wu C and Hao H (2005), "Modeling of simultaneous ground shock and airblast pressure on nearby structures from surface explosions", *International Journal of Impact Engineering*, 31(6), pp. 699-717. <https://doi.org/10.1016/j.ijimpeng.2004.03.002>.
54. IS 1905(1987), "Indian standard code of practice for structural use of unreinforced masonry", *Bureau of Indian Standards* (BIS), New Delhi, India.
55. SP 20(1991), "Handbook on Masonry Design and Construction", Bureau of Indian Standards (BIS), New Delhi, India.
56. Masia M. J., Simundic G., and Page A. W. 2012, "Assessment of the AS3700 relationship between shear bond strength and flexural tensile bond strength in unreinforced masonry", *15th International Brick and Brick Masonry Conference*, Brazil.
57. Al-Dala'ien, R. N., Syamsir, A., Usman, F., & Abdullah M. J. (2023). The effect of the W-shape stirrups shear reinforcement on the dynamic behavior of RC flat solid slab subjected to the low-velocity impact loading. *Results in Engineering*, vol. 19, p. 101353, Sep. 2023, doi: 10.1016/j.rineng.2023.101353.
58. Al-Dala'ien, R. N., Syamsir, A., Abu Bakar, M. S., Usman, F., & Abdullah, M. J. (2023). Failure Modes Behavior of Different Strengthening Types of RC Slabs Subjected to Low-Velocity Impact Loading: A Review. *Journal of Composites Science*, vol. 7, no. 6, p. 246, Jun. 2023, doi: 10.3390/jcs7060246.